Available online at www.sciencedirect.com
ScienceDirect
Journal of Catalysis 254 (2008) 110–120
JOURNAL OF CATALYSIS
www.elsevier.com/locate/jcat

New reaction of anion radicals O^- with water on the surface of FeZSM-5

Gennady I. Panov *, Eugeny V. Starokon, Larisa V. Pirutko, Eugeny A. Paukshtis, Valentin N. Parmon

Boreskov Institute of Catalysis SB RAS, Novosibirsk, Russia

Received 17 September 2007; revised 5 December 2007; accepted 5 December 2007

Available online 8 January 2008

Abstract

Complexes of bivalent iron stabilized in the FeZSM-5 zeolite matrix (α-sites) are known to be able to decompose nitrous oxide stoichiometrically to form oxygen anion radicals, O^-, bound to iron (α-oxygen),

$$(Fe^{II})_\alpha + N_2O \rightarrow (Fe^{III}\text{–}O^-)_\alpha + N_2.$$

Similar to O^- radicals on V and Mo oxides, α-oxygen is highly reactive in respect to CO, H_2, methane and other hydrocarbons. It participates in catalytic oxidation of benzene to phenol by nitrous oxide, providing selectivity close to 100%. In this work, adsorption measurements, IR spectroscopy, TPD, and isotope methods were used to describe an earlier unknown reaction of O^- species with water, which proceeds at 5–200 °C via the hydrogen abstraction mechanism according to the equation

$$2(Fe^{III}\text{–}O^-)_\alpha + H_2O \rightarrow 2(Fe^{III}\text{–}OH^-)_\alpha + (1/2)O_2.$$

The reaction leads to the hydroxyl groups formed on α-sites, and equivalent amount of O_2 evolves into the gas phase from water. Desorption of the hydroxyl groups occurs at above 400 °C via their recombination into water and dioxygen, resulting in the reactivation of α-sites,

$$2(Fe^{III}\text{–}OH^-)_\alpha \rightarrow 2(Fe^{II})_\alpha + H_2O + (1/2)O_2.$$

High sensitivity of α-oxygen to water admixtures may be an important factor explaining some contradictory results reported in the literature on the behavior of α-oxygen. Because α-oxygen is a typical representative of anion radicals O^-, this reaction may be relevant not only to the conventional oxidation catalysis over zeolites and metal oxides, but also to photocatalytic processes, where formation of O^- is well documented.

Keywords: N_2O; α-Oxygen; FeZSM-5; DRIFT spectroscopy; Anion radical O^-; Photocatalytic oxidation

1. Introduction

Over the last decade, FeZSM-5 zeolites have attracted considerable attention in oxidation catalysis, particularly for reactions involving nitrous oxide (N_2O). The zeolites are very efficient for the selective oxidation of aromatics [1,2], N_2O decomposition [3,4], and N_2O reduction by ammonia, methane, and other hydrocarbons [4–8]. A distinctive feature of FeZSM-5 zeolites is the presence of the so-called "α-sites," special mononuclear complexes of bivalent iron Fe(II) stabilized in the zeolite matrix. Due to the pairwise arrangement, α-sites are identified by Mössbauer spectroscopy as binuclear species with the spectral parameters close to those of binuclear iron sites of methane monooxygenases [9–12]. The α-sites are not oxidized by dioxygen but are readily oxidized by nitrous oxide to form anion radicals, O^-, bound to the iron, $(Fe^{III}\text{–}O^-)_\alpha$ [11,13–15],

$$(Fe^{II})_\alpha + N_2O \rightarrow (Fe^{III}\text{–}O^-)_\alpha + N_2. \quad (1)$$

The $Fe^{III}\text{–}O^-$ species could be expected to coexist with the resonance $Fe^{IV}{=}O$ form; however, neither Mössbauer nor RIXS spectroscopy [16] detected the Fe(IV) state in the FeZSM-5. A theoretical consideration of parameters that may control the $Fe^{III}\text{–}O^- \leftrightarrow Fe^{IV}{=}O$ transition was reported by Malykhin et al. [17].

* Corresponding author.
E-mail address: panov@catalysis.nsk.su (G.I. Panov).

0021-9517/$ – see front matter
doi:10.1016/j.jcat.2007.12.001

The O^- radicals on FeZSM-5 are called α-oxygen and denoted herein as O_α. The deposition of O_α is performed by reaction (1) in the temperature range of 200–250 °C. At higher temperature, α-oxygen is unstable, being desorbed into the gas phase as O_2, which leads to the initial bivalent state of α-sites,

$$2(Fe^{III}–O^-)_\alpha \rightarrow 2(Fe^{II})_\alpha + O_2. \quad (2)$$

Similarly to O^- radicals on V and Mo oxides [18–21], α-oxygen has a remarkably high reactivity. Stoichiometric oxidation of methane and other hydrocarbons by α-oxygen occurs readily at room temperature, leading to selective formation of hydroxylated products extracted from the surface of FeZSM-5 [22–25]. α-Oxygen has been shown to participate in catalytic reactions as well. In particular, O_α provides the catalytic oxidation of benzene to phenol by N_2O proceeding at 300–450 °C with selectivity close to 100% [26,27].

The involvement of O_α in the selective oxidation reactions restores interest in an earlier-suggested idea assuming an important role of O^- radicals in oxidation catalysis [19–21,28,29]. This idea has not been generally accepted due to a lack of reliable experimental support. A recent study [13] proposed that O^- radicals, which have a pronounced tendency toward hydrogen abstraction, may serve as universal agents for the activation of molecules to oxidation. This proposal also has sparked additional interest in FeZSM-5. Along with their practical importance, these zeolites provide a convenient model for studying the chemistry of O^- radicals, the concentration of which may be 2–3 orders of magnitude higher in the zeolite system than in conventional oxide systems.

Despite the numerous theoretical [17,30–34] and experimental [35–50] works devoted to the α-sites and α-oxygen, some important points remain subject to debate. In particular, data in the literature on the catalytic properties of FeZSM-5 and the reactivity and thermal stability of α-oxygen differ significantly and are sometimes contradictory. These differences hardly can be attributed to differences in catalyst preparation; more likely, they are due to differing experimental conditions, particularly in admixtures of water.

The role of water has been explored in depth, particularly in studies of the comparatively simple reaction of the decomposition of N_2O to N_2 and O_2. El-Malki et al. [51] reported that water introduced into the feed mixture caused a considerable decrease in the rate of N_2O decomposition. Zhu et al. [52] reported that water may convert active iron species into inactive oxide clusters, Fe_xO_y. Pirngruber and Roy [53], using a step-response technique, found that the high initial activity of FeZSM-5 decayed slowly to the much lower steady-state activity, which they attributed to the poisoning effect of water admixtures strongly adsorbed on the active sites.

Modeling the kinetics of the N_2O decomposition, Heyden et al. [54] demonstrated that water can significantly increase the activation energy of the reaction. An analysis of the literature data leads to the conclusion that the contradictory results obtained by different groups can be consistently explained by the different concentrations of admixed water in the various studies.

An especially interesting effect of water was reported by Bulushev et al. [55]. When feeding H_2O pulses at 250 °C to the FeZSM-5, which contains α-oxygen, these authors observed the evolution of O_2 into the gas phase. The amount of O_2 evolved was about 25% of the amount of α-oxygen.

The foregoing results demonstrate an important (but still not quite clear) role of water that merits further mechanistic investigation. In the present work, we used the adsorption measurements, IR spectroscopy, TPD, and oxygen isotopes to study in detail the interaction of water with both vacant α-sites and sites with adsorbed α-oxygen. This allowed us to discover a new reaction of α-oxygen with water, which may be important not only for the zeolites, but also for other systems in which anion radicals, O^-, can form.

2. Experimental

2.1. Sample

The zeolite ($SiO_2/Al_2O_3 = 72$; 0.53 wt% Fe) was synthesized hydrothermally, with the iron introduced into the initial gel as $FeCl_3$. According to the XRD data, the zeolite crystallinity exceeded 95%. The sample was converted to the H-form by exchange with ammonia buffer, followed by calcination in air at 550 °C. To increase the concentration of α-sites, C_α, the sample also was activated by calcining in vacuum at 900 °C for 1 h. In the activated sample, $C_\alpha = 18 \times 10^{18}$ sites/g.

2.2. Vacuum setup

The experiments were conducted in a stainless steel vacuum static setup providing a vacuum of 10^{-7} Torr. Being isolated, the reaction volume can maintain the vacuum at 10^{-3} Torr overnight. This prevents leakage of the air during experiments and allows reliable adsorption measurements.

The pressure of reaction gases was controlled by two Baratron absolute pressure gauges (MKS Instruments) covering a range of 0.002–100 Torr. The gas-phase composition was controlled by mass spectrometry using a PPT quadrupole residual gas analyzer (MKS Instruments) calibrated with the gas mixtures of known composition.

The setup comprises two quartz reactors, a working reactor and an auxiliary reactor. Each reactor can be easily isolated from the rest part of the reaction volume. The working reactor (6.5 cm^3) was charged with a catalyst, the auxiliary reactor (25 cm^3) was used for various subsidiary functions, particularly for freezing out N_2O, CO_2, water, and so on. An important feature of the working reactor is its negligibly small volume compared with the total reaction volume of the setup (715 cm^3). This allows replacing the gas phase in the setup in a closed reactor without disturbing the adsorption state of the sample established by an earlier treatment. A small amount of the gas remaining in the reactor usually does not impede the next experiment, thus significantly enhancing the reliability of kinetic and adsorption measurements.

2.3. α-Oxygen deposition

A FeZSM-5 sample (0.4 g) was loaded into the reactor as a 0.25–0.5 mm fraction and subjected to a standard pretreatment that included heating at 550 °C under the following conditions: 1 h in vacuum, 1.5 h in oxygen at $P(O_2) = 2$ Torr, 20 min in vacuum, and 20 min in oxygen at $P(O_2) = 0.6$ Torr, followed by cooling in the oxygen to the required temperature.

The standard pretreatment results in careful removal of organic impurities and water and provides full oxidation of the iron fraction that can be oxidized by dioxygen. The latter effect is essential for future correct measurements of α-oxygen.

The deposition of α-oxygen on FeZSM-5 sample was provided by the N_2O decomposition at 240 °C at the initial pressure of 0.6 Torr. Under these conditions, the decomposition proceeded stoichiometrically according to Eq. (1) and was completed within 30 min. To determine the amount of α-oxygen deposited, $N(O_\alpha)$, and thus also the α-site concentration, we followed methods described elsewhere [26]. As an indirect method, the amount of the N_2O decomposed was used, usually registered as the amount of dinitrogen evolved, $N(N_2)$. The direct methods included two low-temperature test reactions based on a specifically high reactivity of α-oxygen: the isotope exchange with O_2,

$$(^{16}O)_\alpha + {}^{18}O_2 \rightarrow (^{18}O)_\alpha + {}^{16}O{}^{18}O, \tag{3}$$

and the CO oxidation,

$$CO + (O)_\alpha \rightarrow (\,)_\alpha + CO_2. \tag{4}$$

Both of these reactions can proceed quickly at room temperature. However, to save time needed for cooling and heating the sample, the reactions were conducted at 100 °C. In the absence of O_α, O_2 isotope exchange becomes noticeable at 400 °C, whereas CO oxidation becomes apparent at above 200 °C.

Within the limits of experimental error (±10%), all 3 methods tested gave the same results. In most cases, we used the $N(N_2)$ value and the data obtained with O_2 isotope exchange. These methods allow a nondestructive quantification of α-oxygen that can be used in further experiments.

For convenience, we designate the initial sample with the vacant α-sites as □/FeZSM-5, and the sample with the α-sites occupied by α-oxygen as O_α/FeZSM-5. Note that the oxidation state of iron is Fe(II) in the first case and Fe(III) in the second case.

2.4. Temperature-programmed desorption (TPD)

Unlike in a flow setup, in our case the TPD experiments were performed in a closed reaction volume, with a temperature ramp of 10 °C/min. The gas phase was controlled by a mass spectrometer (O_2, N_2O, NO, NO_2, CO, CO_2) and a Baratron. To improve heat conductivity under vacuum condition and provide uniform temperature in the samples, the reaction volume was filled with 0.3 Torr of helium. For a graphical representation of the TPD data, the signals of the mass spectrometer and Baratron were converted into the differential form.

2.5. Experiments with H_2O

Water adsorption was performed at the initial H_2O pressure ranging from 2 to 6 Torr, depending on the temperature (5–200 °C). In all cases, on termination of adsorption, the residual water pressure persisted at 0.2–0.5 Torr. In water adsorption on the O_α/FeZSM-5 sample, O_2 was observed to evolve into the gas phase. To determine the amount and isotope composition of the O_2, water was preliminary frozen out to the auxiliary reactor cooled by liquid nitrogen.

To decrease H_2O adsorption on the walls of the setup, the latter was heated to 80 °C. Heating to a higher temperature was undesirable, because in the presence of H_2O this causes some loss of O_2 due to its interaction with copper gaskets [14]. Other details are given below together along the experimental data.

2.6. IR study

To obtain the diffuse reflection spectra, the FeZSM-5 sample (∼0.5 g) was placed into a quartz cell attached to the vacuum setup instead of to the working reactor. This allowed us to conduct various pretreatments of the sample identical to the pretreatments applied in the other experiments, making it possible to compare the IR data with the data from adsorption measurements.

The IR spectra were recorded at room temperature using a Fourier spectrometer (Shimadzu 8300) in the range of 2100–6000 cm^{-1} with 2-cm^{-1} resolution. A total of 50 scans were obtained for the spectra accumulation. A tailor-made holder provided an accurate position of the cell relative to the beam. Deviation of the baseline at 6000 cm^{-1} did not exceed 15% in the various experiments, allowing us to obtain reproducible results over the entire spectral region. The spectra were converted to the Kubelka–Muna $F(R)$ scale: $F(R) = (1-R)^2/2R$. The sample pretreatment conditions before the spectra were obtained are described in the next section.

3. Results

3.1. TPD characterization of α-oxygen

Before studying the interaction of H_2O with α-oxygen, we conducted some experiments on α-oxygen deposition and its characterization by TPD. Fig. 1 shows the TPD curves of α-oxygen obtained after stoichiometric decomposition of N_2O at 240 °C [Eq. (1)] for 1, 2, and 30 min under an initial N_2O pressure 0.6 Torr. It can be seen that the amount of α-oxygen increases with time, with the peak maximum shifting to a low-temperature region, from 380 to 365 °C. This shift may be caused by the increased surface concentration of O_α atoms, which facilitates their recombination in the gas phase. A further increase in the reaction time to 90 min affects neither the intensity of the O_2 peak nor the temperature of its maximum. The amount of O_α measured by the TPD agrees well with the $N(O_\alpha)$ value measured by other methods.

Note that at a higher N_2O pressure (e.g., 10 Torr) and increased reaction time, N_2O decomposition may lead to some

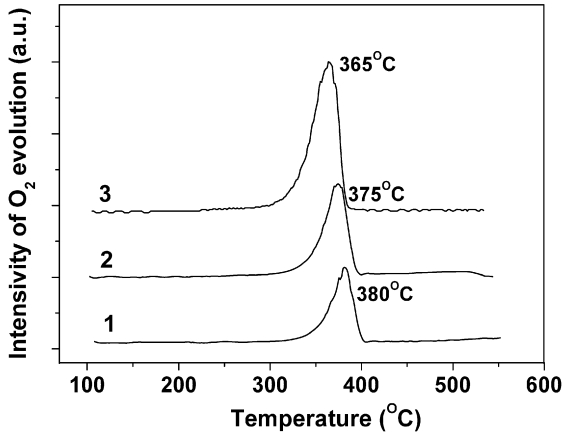

Fig. 1. TPD of α-oxygen deposited from N_2O at 240 °C during different reaction times: (1) 1 min (10×10^{18} atom/g); (2) 2 min (13×10^{18} atom/g); (3) 30 min (18×10^{18} atom/g).

decrease in the $N(O_\alpha)$ value and the appearance of NO and NO_2 in the TPD products. The formation of NO_x on the surface of FeZSM-5 has been reported in a number of works. According to Novakova and Sobalik [49], it results from slow N_2O reaction with α-oxygen. Under the conditions of O_α deposition used in this work, no formation of NO_x occurred, and no mass numbers 30 and 46 were registered at the TPD within the limits of accuracy of mass spectrometry.

3.2. Interaction of water with vacant α-sites of □/FeZSM-5

These experiments were conducted in the following manner. The □/FeZSM-5 sample was deactivated by water adsorption at 4 Torr and 100 °C for 40 min. Then reactivation of the α-sites was performed by desorption of H_2O at different temperatures. For this, the sample was evacuated for 1 h with a stepwise temperature increase from 240 to 550 °C. In parallel experiments, the effect of H_2O desorption on the state of α-sites was tested by two methods: using N_2O decomposition to estimate α-site reactivation with respect to O_α deposition, and taking the IR spectra to register the OH groups that remain adsorbed on the α-sites. In the first method, after evacuation at a chosen temperature, the sample was cooled to 240 °C for O_α deposition, and its amount was measured. In the second method, the sample was cooled to room temperature, and the IR cell was transferred to the spectrometer to obtain the spectra.

3.2.1. Reactivation of α-sites

The data in Table 1 demonstrate that the adsorption of H_2O on the □/FeZSM-5 sample had a significant deactivating effect. Evacuation at 240 °C reactivated only ca. 10% of the α-sites (2×10^{18} atom/g). The reactivation was quickly enhanced by elevating the evacuation temperature. At 450 °C, nearly all of the sites became active, providing the value of $N(O_\alpha) = 17 \times 10^{18}$ atom/g on α-oxygen deposition.

Two unusual results stand out in Table 1, especially in the case of experiment 1, which had the lowest evacuation temperature: (1) The amount of N_2O decomposed at O_α deposition exceeded 5–6 times the amount of α-oxygen registered by the

Table 1
Effect of evacuation temperature on reactivation of α-sites after water adsorption on □/FeZSM-5

Exp. No.	Evacuation temperature (°C)	Amount of N_2O decomposed (10^{18} molecule/g)	Amount of O_2 evolved at N_2O decomposition (10^{18} atom/g)	Amount of O_α registered (10^{18} atom/g)
1	240	11	3.0	2
2	350	16	1.5	13
3	400	17	0.8	15
4	450	18	0.4	17
5	500	19	0.6	18
6	550	19	0.8	18

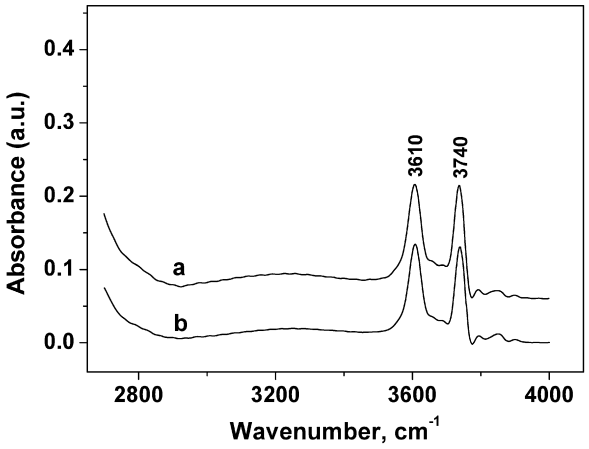

Fig. 2. IR spectra of FeZSM-5 after standard pretreatment at 550 °C (a) and subsequent deposition of α-oxygen (b).

test reactions, and (2) some evolution of O_2 into the gas phase occurred at the N_2O decomposition. These phenomena, not previously reported, are certainly caused by water; we discuss the mechanistic reason for this later.

3.2.2. IR data

Fig. 2 shows the spectrum of the FeZSM-5 sample in the vibrational region of hydroxyl groups, obtained after the standard pretreatment (spectrum a). The spectrum contains two absorption bands (a and b), corresponding to the bridging OH groups Si–OH–Al (3610 cm^{-1}) and terminal Si–OH groups (3740 cm^{-1}). This spectrum is typical of the standard state of the sample, and we use it here as a reference for comparing the spectra obtained in the experiments with H_2O. Note that deposition of α-oxygen did not change the spectrum (Fig. 2, spectrum b).

Fig. 3 shows the spectra obtained after H_2O adsorption at 100 °C followed by stepwise evacuation at different temperatures. After evacuation at 240 °C (spectrum a), a broad signal at 2900–3500 cm^{-1} was observed, indicating the presence of physically adsorbed water. In the region of OH vibrations, along with the previously observed absorption bands at 3610 (a) and 3740 cm^{-1} (b), an intense new signal appeared at 3665 cm^{-1}. The position of the signal is close to the signal at 3670 cm^{-1} observed earlier for the OH groups that formed on interaction of H_2 and O_α [56,57]. The intensity of this signal rapidly

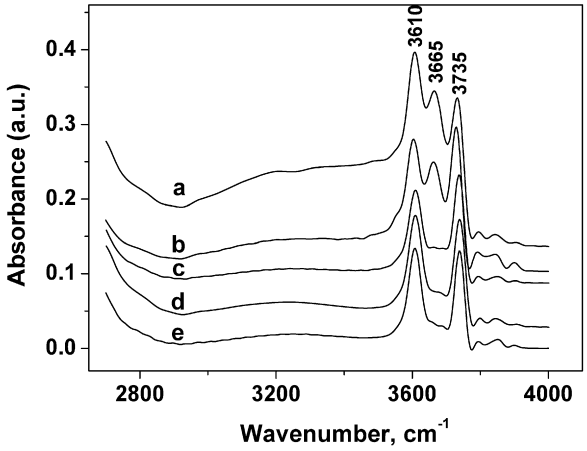

Fig. 3. IR spectra taken after H_2O adsorption on □/FeZSM-5 at 100 °C and subsequent evacuation at different temperatures: 240 °C (a), 350 °C (b), 450 °C (c), 500 °C (d), 550 °C (e).

decreased with increasing evacuation temperature. At 450 °C (spectrum c), it became practically imperceptible, making the spectrum close to that of the standard sample (Fig. 2).

The foregoing data demonstrate that water adsorption proceeded by a dissociative mechanism and led to the formation of hydroxyl groups adsorbed on α-sites and their eventual deactivation. Removing these groups by evacuation resulted in reactivation of α-sites. The adsorption of water can be represented by the following equation:

$$(Fe^{II})_\alpha + H_2O + Z \rightarrow (Fe^{II}\text{–}OH)_\alpha + ZH, \quad (5)$$

where Z is some adsorption site on the zeolite surface. Note that according to the Mössbauer data, the oxidation state of iron on H_2O adsorption remained unchanged [11]. Keeping the FeZSM-5 samples for 20 h in a water saturated air at 25 °C led to no effect: the □/FeZSM-5 sample retained its initial iron state Fe(II), and the O_α/FeZSM-5 sample retained the iron state Fe(III).

3.3. Interaction of water with O_α/FeZSM-5

The original intent in the present study was to characterize the OH groups formed on O_α/FeZSM-5 on H_2O adsorption and evaluate the effect of α-site reactivation on the stepwise evacuation of the sample. However, water adsorption on the O_α/FeZSM-5 produced a remarkable phenomenon—the evolution of O_2 into the gas phase—which, the best of our knowledge, has not yet been reported with conventional systems. Therefore, we first thoroughly investigated this phenomenon.

3.3.1. O_2 evolution

As in the previous case, the first experiment was conducted at 100 °C. Water adsorption on the O_α/FeZSM-5 with $N(O_\alpha) = 18 \times 10^{18}$ O_α atoms/g (Table 2, run 1) led to the evolution of O_2 in the amount of 8×10^{18} O atoms/g. We performed a TPD experiment to characterize the state of α-oxygen after water adsorption. During this experiment, water was frozen out into an auxiliary reactor cooled with liquid nitrogen. The amount of O_2 was measured using the mass spectrometer and the Baratron. As

Table 2
Evolution of O_2 at water adsorption on O_α/FeZSM-5 at different temperatures and in subsequent TPD experiments

Exp. No.	Initial amount of O_α (10^{18} atom/g)	Temperature of H_2O adsorption (°C)	H_2O pressure (Torr)	Amount of O_2 evolved (10^{18} atom/g)	
				H_2O adsorption	TPD
1	18	100	2	8.0	9.0
2	17	25	4	8.0	8.5
3	17	50	4	7.0	7.0
4	17	125	2	7.0	9.0
6	18	200	2	7.0	9.0
Average	17.4 (100%)			7.4 (43%)	8.5 (49%)

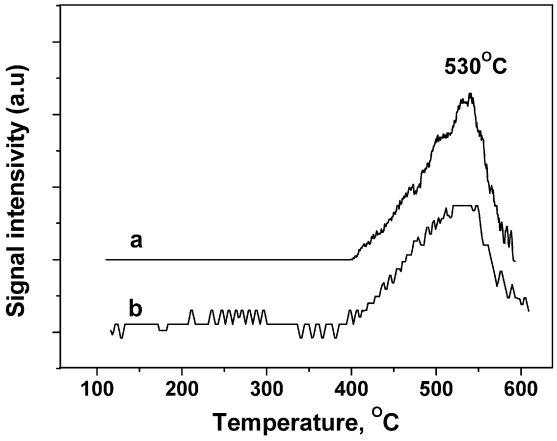

Fig. 4. TPD of O_2 after H_2O adsorption on O_α/FeZSM-5 at 100 °C and subsequent evacuation at 240 °C: mass spectrometer data (a); Baratron data (b).

can be seen in Fig. 4, both instruments give a similar picture, with the maximum O_2 peak near 530 °C. The amount of O_2, the sole desorption product, was 9×10^{18} O atoms/g (Table 2). Thus, the total amount of O_2 evolved was close to the initial amount of $N(O_\alpha)$, and its evolution occurred in two approximately equal portions: one portion at the adsorption of water and the other portion at the TPD.

To obtain more information, we conducted a number of similar experiments, varying the temperature of H_2O adsorption from 25 to 200 °C. As shown in Table 2, we found that the amount of O_2 evolved did not depend on the temperature and in all cases was 40–47% of the initial amount of O_α. Approximately the same amount of O_2 evolved in the subsequent TPD experiments. The averaged data demonstrate that if the $N(O_\alpha)$ value was taken as 100%, then the amount of O_2 evolved at the H_2O adsorption was equivalent to 43%, and the amount of O_2 evolved at TPD was 49%. Despite our efforts to provide the most accurate measurements, the values of $N(O_2)$ on H_2O adsorption seem to be underestimated somewhat, possibly due to partial capture of O_2 as water freezes. We proceed based on the assumption that both H_2O adsorption and TPD evolve identical portions of O_2, with each portion equal to $(1/2)N(O_\alpha)$. Note that water adsorption makes the O_α/FeZSM-5 sample inert toward the test reactions, with both O_2 isotope exchange and CO oxidation no longer occurring.

Table 3
Effect of evacuation temperature on the reactivation of α-sites after water adsorption on O_α/FeZSM-5

Exp. No.	Evacuation temperature (°C)	Amount of N_2O decomposed (10^{18} molecule/g)	Amount of O_α registered (10^{18} atom/g)
1	240	3	1
2	400	6	5
3	450	12	11
4	500	17	16
5	550	19	18

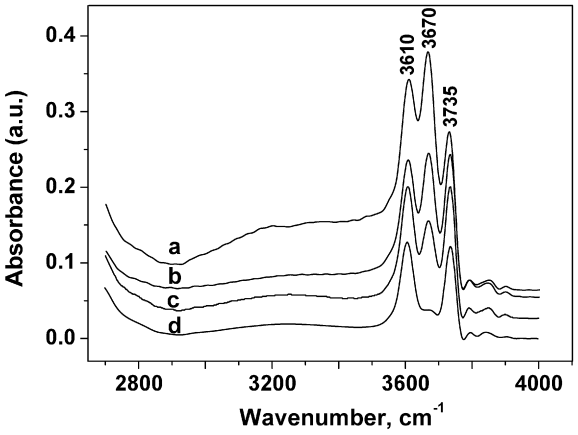

Fig. 5. IR spectra taken after H_2O adsorption on O_α/FeZSM-5 at 100 °C and subsequent evacuation at different temperatures: 240 °C (a), 450 °C (b), 500 °C (c), and 550 °C (d).

3.3.2. Reactivation of α-sites

Table 3 gives the data on the α-site reactivation resulting from evacuation of $H_2O + O_\alpha$/FeZSM-5 at different temperatures. In this case, the reactivation appeared to be much more difficult compared with reactivation of the sample with vacant α-sites. In particular, whereas evacuation of the $H_2O + \square$/FeZSM-5 at 400 °C reactivated 15×10^{18} sites/g (Table 1, run 3), evacuation of $H_2O + O_\alpha$/FeZSM-5 at the same temperature (Table 3, run 2) reactivated only 5×10^{18} sites/g, with full reactivation in the latter case occurring only at 550 °C.

3.3.3. IR data

Fig. 5 shows the spectra obtained after water adsorption on O_α/FeZSM-5 at 100 °C and subsequent stepwise evacuation of the sample at different temperatures. Similar to the situation for the $H_2O + \square$/FeZSM-5 sample, here the spectra also contain three absorption bands in the OH vibrational region. Two of these bands (3610 and 3735 cm^{-1}) correspond to the bridging (Si–OH–Al) and terminal (Si–OH) hydroxyl groups of the zeolite matrix, whereas the band at 3670 cm^{-1} is assigned to the hydroxyls on the oxidized α-sites, $(Fe^{III}–OH^-)_\alpha$. This band had a much higher thermal stability than the band at 3665 cm^{-1} on the $H_2O + \square$/FeZSM-5 sample (Fig. 3). It retained considerable intensity even at 500 °C, and only evacuation at 550 °C could lead to spectrum d, which is similar to the spectrum of samples in the standard state (Fig. 2).

Comparing the results shown in Fig. 5 with the data of Table 3 for the $H_2O + O_\alpha$/FeZSM-5 sample reveals a correlation between the decreasing intensity of a.b. 3670 cm^{-1} and the increasing fraction of the reactivated α-sites.

4. Discussion

4.1. Identification of the process evolving O_2

4.1.1. Competitive adsorption or chemical reaction?

As noted above, the evolution of O_2 from the O_α/FeZSM-5 surface on H_2O adsorption was reported earlier by Bulushev et al. [55]. These authors explained this unusual phenomenon by the competitive nature of water adsorption, which can be described by the following equation:

$$(Fe^{III}–O^-)_\alpha + H_2O + Z \rightarrow (Fe^{II}–OH)_\alpha + ZH + (1/2)O_2. \quad (6)$$

The OH groups generated from water occupy α-sites and displace α-oxygen into the gas phase. Because water is unable to oxidize α-sites [11], displacement of O_α implies the reduction of active iron, Fe(III) → Fe(II), as in the case of thermal desorption of α-oxygen [Eq. (2)].

At first glance, such an explanation seems quite plausible; however, our results raise two difficult questions: (1) Why does water displace only 1/2 of α-oxygen? and (2) why does the remaining O_α desorb at 530 °C instead of the usual 370 °C? These difficulties disappear if we assume the reactivity of α-oxygen to be so high that it can enter chemical reaction with water to oxidize it as a one-electron oxidant,

$$2(Fe^{III}–O^-)_\alpha + H_2O \rightarrow 2(Fe^{III}–OH^-)_\alpha + (1/2)O_2. \quad (7)$$

In this reaction, α-oxygen abstracts the hydrogen from H_2O and turns into the OH groups bonded to α-sites (a.b. 3670 cm^{-1}). According to the stoichiometry of reaction (7), the amount of dioxygen evolved from water should be 1/2 of $N(O_\alpha)$, which was observed experimentally. The evolution of the second part of O_2, as recorded in the TPD runs, occurs due to dehydroxylation of α-sites, yielding water and dioxygen,

$$2(Fe^{III}–OH^-)_\alpha \rightarrow 2(Fe^{II})_\alpha + H_2O + (1/2)O_2. \quad (8)$$

Unlike a conventional dehydroxylation process, at which two OH-groups yield an H_2O molecule and a bridging oxygen atom on the surface [58], the dehydroxylation of α-sites shown in Eq. (8) leads to the desorption of oxygen and the reduction of the iron. This is confirmed by the data on the reactivation of α-sites as well as by the IR spectra indicating disappearance of the hydroxyl groups bonded to α-sites.

The evolution of oxygen on H_2O adsorption [Eq. (7)] is the most interesting phenomenon, demonstrating very strong ability of α-oxygen to perform hydrogen abstraction. This ability of anion radicals O^- is well known, because hydrogen abstraction occurs at the interaction of O^- with methane and other hydrocarbons on V and Mo oxides [18–20] as well as on the FeZSM-5 [56,57]. Therefore, the same type reaction of O_α with water is in line with the aforementioned patterns, but still it seems a quite unusual process for which additional evidence would be useful.

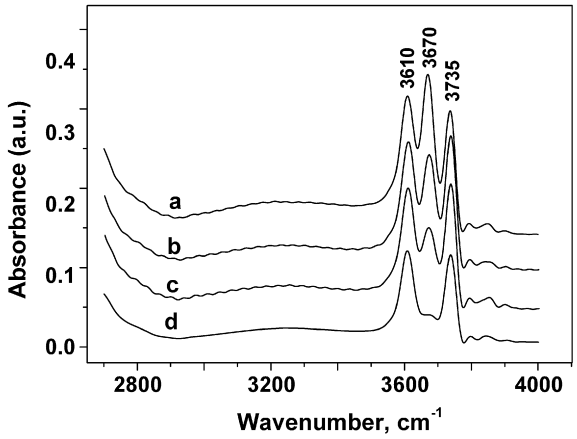

Fig. 6. IR spectra taken after H_2 interaction with O_α/FeZSM-5 at 100 °C and subsequent evacuation at different temperatures: 240 °C (a), 450 °C (b), 500 °C (c), and 550 °C (d).

Table 4
Effect of evacuation temperature on reactivation of α-sites after H_2 interaction with O_α/FeZSM-5

Exp. No.	Evacuation temperature (°C)	Amount of N_2O decomposed (10^{18} molecule/g)	Amount of O_α registered (10^{18} atom/g)
1	240	3	2
3	450	13	11
4	500	17	16
5	550	19	18

4.1.2. Comparison of OH groups of various origin

The properties of $(Fe^{III}–OH^-)_\alpha$ hydroxyl groups formed by reaction (7) may provide such additional evidence. If these groups actually form due to the hydrogen abstraction from H_2O, then they should be identical to the OH groups formed by the reaction of H_2 with α-oxygen,

$$H_2 + 2(Fe^{III}–O^-)_\alpha \rightarrow 2(Fe^{III}–OH^-)_\alpha. \quad (9)$$

Reaction (9) has been carefully investigated in previous studies [56,57], including measurement of the H_2/D_2 kinetic isotope effect. In the present work, we conducted this reaction to study the spectral and thermal characteristics of the OH groups formed and to compare them with the OH groups formed in the H_2O + □/FeZSM-5 and H_2O + O_α/FeZSM-5 systems.

Fig. 6 shows the IR spectra obtained with the H_2 + O_α/FeZSM-5 sample. It can be seen that the reaction of hydrogen with O_α gave rise to an intense a.b. 3670 cm^{-1} related to the formation of OH groups on α-sites. Evacuation of the sample as the temperature increased led to quite a slow decrease in the intensity of this band (spectra a, b, and c). Complete disappearance of the band occurred only at 550 °C (spectrum d), demonstrating the high thermal stability of the OH groups, similar to that of the OH groups on the H_2O + O_α/FeZSM-5 sample (Fig. 5).

Table 4 shows the effect of evacuation temperature on the reactivation of α-sites tested by O_α deposition. This reactivation required high temperatures. Complete restoration of the activity providing $N(O_\alpha) = 18 \times 10^{18}$ atom/g occurred only at 550 °C.

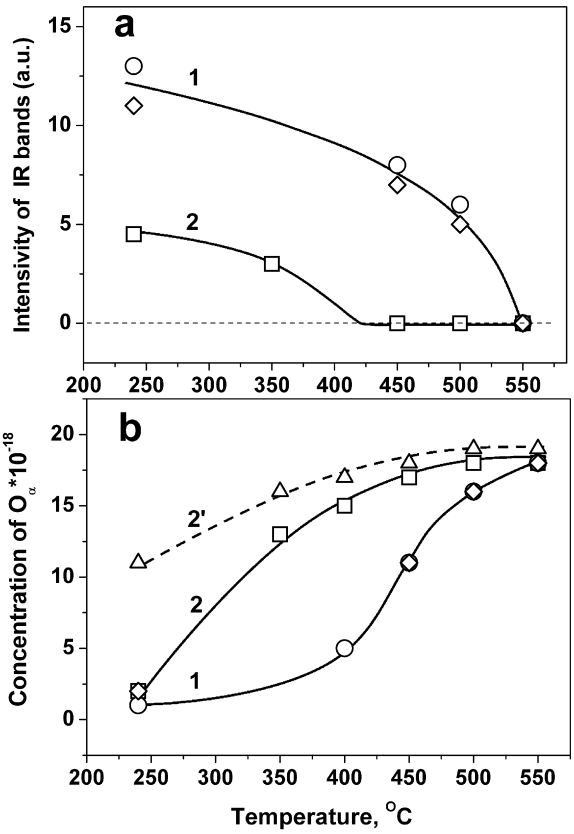

Fig. 7. Effect of evacuation temperature on the IR intensity of $(OH)_\alpha$ groups (a) and the reactivation of α-sites (b) for different reaction systems: H_2O + O_α/FeZSM-5 (○); H_2O + □/FeZSM-5 (□); H_2 + O_α/FeZSM-5 (◇). The dotted line represents corrected dependence for the system H_2O + □/FeZSM-5 (see text).

The TPD experiment performed after the H_2 + O_α/FeZSM-5 sample was evacuated at 240 °C gave a picture (not shown) identical to that shown in Fig. 4 for the H_2O + O_α/FeZSM-5 sample. O_2 evolution also exhibited a peak with the maximum at 530 °C.

We now have all of the experimental data needed to compare the spectral and thermal characteristics of the OH groups of various origin formed on the H_2O + □/FeZSM-5, H_2O + O_α/FeZSM-5, and H_2 + O_α/FeZSM-5 samples. Comparing of the IR spectra (Figs. 3, 5, and 6) demonstrates that a.b. 3670 cm^{-1} on the H_2O + O_α/FeZSM-5 sample coincides with the corresponding band on the H_2 + O_α/FeZSM-5 sample. But because the hydroxyl groups on the H_2O + □/FeZSM-5 sample have a close absorption maximum (3665 cm^{-1}), it may be concluded that the nature of OH groups has only a slight affect on the position of their absorption bands.

Comparing the thermal stability of the OH groups provides much more informative findings. Fig. 7a shows the IR band intensities obtained by deconvolution of spectra in Figs. 3, 5, and 6 versus the evacuation temperature. The experimental results are described by two different dependencies. The OH groups formed in the H_2O + O_α/FeZSM-5 and H_2 + O_α/FeZSM-5 systems have a high and similar thermal stability, described by the common dependence 1. In comparison,

Table 5
Fraction of ^{18}O isotope in O_2 evolved upon $H_2{}^{16}O$ adsorption on $^{18}O_\alpha$/FeZSM-5 at different temperatures

Exp. No.	Temperature of H_2O adsorption (°C)	H_2O pressure (Torr)	^{18}O fraction in O_2 (%)
1	5	6	13
3	25	4	21
4	50	4	36
5	100	2	51
6	125	2	59
7	200	2	69

the OH groups in the H_2O + □/FeZSM-5 system have a much lower stability, described by dependence 2.

These IR data should correlate with the reactivation of α-sites, because the OH groups are the cause of the deactivation. Indeed, an increase in the concentration of reactivated sites with increasing evacuation temperature (Fig. 7b) also can be described by two different dependencies plotted using the data in Tables 1, 3, and 4. The "difficult" reactivation of the H_2O + O_α/FeZSM-5 and H_2 + O_α/FeZSM-5 systems described by common dependence 1 differs significantly from the "easy" reactivation of the H_2O + □/FeZSM-5 system described by dependence 2.

The foregoing results lead us to conclude that reactions of both H_2O and H_2 with α-oxygen yield identical hydroxyl groups with similar a.b. in the IR spectra, thermal stability, and relationships to the reactivation of α-sites. Because there is no doubt that the OH groups formed by the reaction with hydrogen include α-oxygen, the OH groups formed by the reaction with water also should include this same oxygen. Therefore, water does not displace the α-oxygen, but rather enters a chemical reaction described by Eq. (6) that proceeds via the transfer of hydrogen to O_α, resulting in the formation of OH groups and the evolution of O_2 into the gas phase.

4.1.3. Isotope studies

Although isotope labeling can provide useful information on the reaction mechanism, the efficiency of this approach is often compromised by independent channels of the label transfer, hampering straightforward interpretation of the results. Regardless, isotope studies are useful in estimating the complexity of a reaction system.

We conducted a number of experiments on the interaction of $H_{16}{}^2O$ with α-oxygen represented by the ^{18}O isotope (97%). Theoretically, dioxygen evolved from water by reaction (7) should contain only the isotope ^{16}O; however, Table 5 shows that the O_2 actually had a mixed isotope composition that varies widely depending on the temperature of water adsorption. As the temperature decreased from 200 to 5 °C, the fraction of "heavy" isotope fell from 69% to 13%. A graphical representation of the result is given in Fig. 8. It can be seen that the ^{18}O fraction retained its tendency to decrease further, striving to zero with extrapolation of the temperature to minus 10–15 °C. This result confirms the water origin of O_2 evolved in the low-

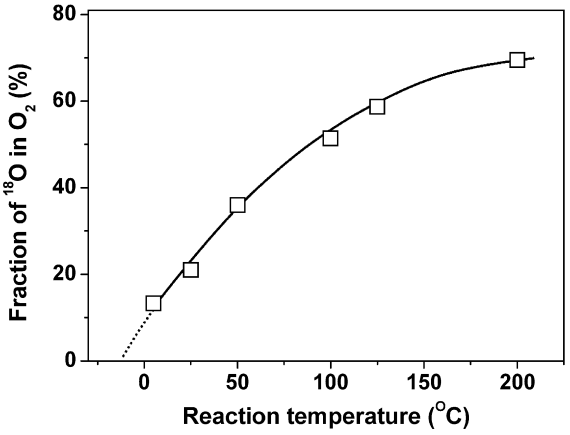

Fig. 8. Fraction of ^{18}O isotope in O_2 evolved by the reaction $H_2{}^{16}O$ + $^{18}O_\alpha$/FeZSM-5 at different temperatures (plotted with the data of Table 5).

temperature region. The following scheme can be suggested as an example of a simplified mechanism of O_2 formation:

$$(Fe^{III}\text{–}{}^{18}O^-)_\alpha + H_2{}^{16}O + Z \rightarrow [Fe^{III}\text{–}{}^{18}O^- \cdots H\text{–}{}^{16}OH] \rightarrow (Fe^{III}\text{–}{}^{18}OH^-)_\alpha + Z^{16}OH, \quad (10)$$

$$2Z^{16}OH \rightarrow [H_2{}^{16}O_2] \rightarrow H_2{}^{16}O + (1/2)^{16}O_2 + 2Z. \quad (11)$$

In the first step, hydrogen is transferred from the water molecule to O_α, resulting in the formation of two hydroxyl groups. One of these groups, ^{18}OH, containing α-oxygen, is bound to the α-site; the other, ^{16}OH, being a remainder of the water molecule, is adsorbed on a zeolite site. In the second step, the interaction of the water-derived ^{16}OH groups occurs via possible formation of intermediate hydrogen peroxide, which decomposes with the evolution of $^{16}O_2$.

The appearance of ^{18}O in the O_2 at higher temperatures indicates that some independent processes of the isotope exchange occur, with the contribution increasing with increasing temperature. The evolved dioxygen isotopomers have a slightly nonequilibrium distribution, with the concentration of $^{16}O^{18}O$ species 5–15 rel% lower than its equilibrium value. This is another indication of the complexity of the reaction occurring in the H_2O + O_α/FeZSM-5 system.

4.2. Effect of water on quantification of α-oxygen

In examining the data in Table 1 (Section 3.2.1), we noted a discordance between the amount of nitrous oxide decomposed, $N(N_2)$, and the amount of α-oxygen deposited, $N(O_\alpha)$, registered by the test reactions. This discordance can be easily explained with regard to the reaction of O_α with H_2O. Theoretically, the deposition of O_α via decomposition of N_2O on the vacant α-sites [Eq. (1)] should always provide the equality $N(N_2) = N(O_\alpha)$. But if water is present in the reaction system, it may convert a part of the O_α into inactive OH groups, thus giving an underestimated $N(O_\alpha)$ value. The discordance between $N(N_2)$ and $N(O_\alpha)$ will increase with the increasing concentration of residual water and decrease with the increasing evacuation temperature, as was shown by our experiments. The same mechanism explains some of the evolution of O_2 on O_α deposition in a "wet" system (Table 1).

Table 6
Summary results for the reaction systems studied

Reaction system	Results of reaction taking place in the system		Temperature of ca. 50% decrease of $(OH)_\alpha$ amount		Results of TPD	
	Amount of O_2 evolved	Formation of $(OH)_\alpha$ groups	IR data	Reactivation	Amount of O_2 evolved	T_{max} (°C)
$H_2O + \square$/FeZSM-5	0.0	3665 cm^{-1} $(Fe^{2+}–OH)_\alpha$	<240	<240	0.0	–
$H_2O + O_\alpha$/FeZSM-5	$(1/2)N(O_\alpha)$	3670 cm^{-1} $(Fe^{3+}–OH^-)_\alpha$	450	430	$(1/2)N(O_\alpha)$	530
$H_2 + O_\alpha$/FeZSM-5	0.0	3670 cm^{-1} $(Fe^{3+}–OH^-)_\alpha$	450	430	$(1/2)N(O_\alpha)$	530

The foregoing considerations lead to some important remarks:

1. Measuring $N(O_\alpha)$ by test reactions may provide correct results only in a "dry" reaction system. Trace amounts of water lead to underestimation of values. This may give the misleading impression, sometimes reported in the literature, that N_2O decomposition on α-sites provides both active and inactive oxygen species.
2. If the reaction system contains H_2O admixtures, then the $N(O_\alpha)$ values can be obtained from the $N(N_2)$ data. In this case, the entire amount of oxygen deposited on the surface may be considered O_α, even if it exhibits no reactivity.

Following this reasoning, we should correct the results on α-site reactivation of the $H_2O + \square$/FeZSM-5 sample, which showed a discordance between the $N(O_\alpha)$ and $N(N_2)$. Fig. 7b, curve 2 describes the reactivation plotted with the $N(O_\alpha)$ values obtained from Table 1, and dotted curve 2′ describes the corrected dependence plotted with the $N(N_2)$ values also obtained from Table 1. The latter curve shows that the reactivation of α-sites in the $H_2O + \square$/FeZSM-5 sample actually proceeded much more easily. Indeed, evacuation at 240 °C reactivated 60% of the α-sites, compared with 10% as demonstrated by the $N(O_\alpha)$ data.

4.3. Comments related to experimental units

High sensitivity of α-oxygen to water can explain a significant part of the conflicting literature data related to both the state of active iron and the properties of O_α. In this respect, an essential distinction in the experimental conditions is related to the type of unit used, that is, a flow unit or a static vacuum unit. At present, due to easy automation and high performance, flow and pulse flow units are widely used for the adsorption and catalytic studies. However, a continuous gas flow through the catalyst bed entails some complications, especially when it is important to minimize contact between the catalyst and small impurities, like the water impurities in our case.

We now make an estimation taking into account some typical experimental parameters for α-oxygen deposition and the measurement of its amount. Assume that a 0.5-g sample with the $C_\alpha = 20 \times 10^{18}$ sites/g is used in the experiments. Thus, the amount of α-oxygen that can be deposited on the sample is 10×10^{18} O_α atoms. If the flow rate through the reactor is 60 cm^3/min, then at 1.5 h time on stream (which is the duration of experiment), the gas volume will constitute 5.4 L. Deactivating 10% of the α-oxygen by reaction (7) requires 5×10^{17} H_2O molecules, corresponding to 3.5×10^{-4} mol% of water in the feed gas. Therefore, correct measurement of $N(O_\alpha)$ is possible only if the water admixture does not exceed 3–4 ppm. Even if we assume that only 10% of the water admixture is involved in the reaction with α-oxygen, this imposes difficult demands on the experiment.

In this respect, a vacuum unit provides a significant advantage. In this case, the amount of gas required for the experiment is about 10^4 times less than that required for a flow unit, and thus impurities are usually not an issue. The concentration of α-oxygen may remain unchanged for several days, and so its properties can be studied reliably.

5. Conclusion

Table 6 summarizes the main results of the present study obtained with different reaction systems. Water adsorption on the vacant α-sites of the $\square$/FeZSM-5 sample [Eq. (5)] led to the hydroxyl groups $(Fe^{II}–OH)_\alpha$ at 3665 cm^{-1}. Evacuation of the sample at 240 °C resulted in a 60% decrease in their amount and, accordingly, in the reactivation of the most of the α-sites. No oxygen evolution was observed in the TPD experiments.

The reaction system $H_2O + O_\alpha$/FeZSM-5 is of great interest. Water adsorption on the oxidized α-sites was accompanied by its chemical reaction with O_α [Eq. (7)] proceeding with the abstraction of hydrogen from H_2O and evolution of O_2 into the gas phase. The amount of O_2 evolved was equal to half of the initial amount of α-oxygen, $(1/2)N(O_\alpha)$. The resulting OH groups, $(Fe^{III}–OH^-)_\alpha$, at 3670 cm^{-1} exhibited high thermal stability; a 50% decrease in their amount occurred only on evacuation at 430–450 °C. According to the TPD results, desorption of the OH groups occurred through their recombination into H_2O and O_2. The amount of O_2 evolved in this process also was equal to $(1/2)N(O_\alpha)$, with $T_{max} = 530$ °C.

It is very significant that identical hydroxyl groups also formed in the $H_2 + O_\alpha$/FeZSM-5 system. As Table 6 shows, these groups have similar spectral and thermal characteristics to the hydroxyls formed in the $H_2O + O_\alpha$/FeZSM-5 system. On TPD, they also desorbed with the evolution of O_2 in the amount of $(1/2)N(O_\alpha)$, with $T_{max} = 530$ °C. Because the hydroxyls in the latter case certainly included the α-oxygen, this finding indicates that O_2 evolving in the $H_2O + O_\alpha$/FeZSM-5 system originated from water rather than from α-oxygen.

The reaction of α-oxygen with water may be of interest not only for the zeolite system studied, but also for other catalytic systems in which formation of anion radicals O^- may occur. Besides conventional oxidation of hydrocarbons over metal ox-

ides, where O^- is assumed to play an important role in the activation of O_2 [14], this reaction may be important for photocatalytic processes, which proceed most efficiently over TiO_2, where UV radiation-induced O^- formation is well documented [59,60].

The evolution of O_2 in the reaction of H_2O with α-oxygen is also associated with the photo-oxidation of water and with chemical models mimicking the water oxidase enzymes [61–66]. The functioning mechanism of these systems, including the nature of intermediate species leading to the formation of O_2, is especially difficult to elucidate. The reaction is usually represented by the following equation:

$$2h^+ + H_2O \rightarrow 2H^+_{aq} + (1/2)O_2, \tag{12}$$

using a formal notion of the "hole" (h^+), with some chemical species having a high electron affinity. The results obtained in our study allow us to assume that the O^- radical can serve as a hole, which, on substitution for the h^+ in Eq. (12), gives an equation similar to Eq. (7) to describe the evolution of O_2 in the system studied in this work.

Some authors consider O^- species a possible form of the active oxygen in biological oxidation with monooxygenases [67]. In this case, the ability of O^- to react with water also may play some role in these systems.

Acknowledgments

The authors thank K.A. Dubkov for help in obtaining the IR spectra and A.V. Khasin, A.A. Shteinman, A.V. Vorontsov, and G.M. Zhidomirov for useful discussions and comments. Financial support was provided by the Russian Foundation for Basic Research (projects 06-03-33087-a and 06-03-72551).

References

[1] G.I. Panov, CATTECH 4 (2000) 18.
[2] V.N. Parmon, G.I. Panov, A. Uriarte, A.S. Noskov, Catal. Today 100 (2005) 115.
[3] F. Kapteijn, J. Rodriguez-Mirasol, J.A. Moulijn, Appl. Catal. B Environ. 9 (1996) 25.
[4] J. Pérez-Ramírez, F. Kapteijn, K. Schöffel, J.A. Moulijn, Appl. Catal. B Environ. 44 (2003) 117.
[5] G. Centi, S. Perathoner, F. Vanazza, M. Marella, M. Tomaselli, M. Mantegazza, Adv. Environ. Res. 4 (2000) 325.
[6] Q. Zhu, B.L. Mojet, R.A.J. Janssen, E.J.M. Hensen, J. van Grondelle, P.C.M.M. Magusin, R.A. van Santen, Catal. Lett. 81 (2002) 205.
[7] S. Komeoka, T. Nobukova, S.-I. Tanaka, I. Shin-ichi, K. Tomishige, K. Kunimori, Phys. Chem. Chem. Phys. 5 (2003) 3328.
[8] T. Nobukawa, K. Sugawara, K. Okumura, K. Tomishige, K. Kunimori, Appl. Catal. B Environ. 70 (2007) 342.
[9] G.I. Panov, V.I. Sobolev, K.A. Dubkov, V.N. Parmon, N.S. Ovanesyan, A.E. Shilov, A.A. Shteinman, React. Kinet. Catal. Lett. 61 (2) (1997) 251.
[10] P. Fejes, K. Lazar, I. Marsi, A. Rockenbauer, L. Korecz, J.B. Nagy, S. Perathoner, G. Centi, Appl. Catal. A 252 (2003) 75.
[11] K.A. Dubkov, N.S. Ovanesyan, A.A. Shteinman, E.V. Starokon, G.I. Panov, J. Catal. 207 (2002) 341.
[12] J. Taboada, A. Overweg, P.J. Kooyman, I.W.C.E. Arends, G. Mul, J. Catal. 231 (2005) 56.
[13] G.I. Panov, K.A. Dubkov, E.V. Starokon, Catal. Today 117 (2006) 148.
[14] E.V. Starokon, K.A. Dubkov, L.V. Pirutko, G.I. Panov, Top. Catal. 73 (2003) 137.
[15] P.K. Roy, G.D. Pirngruber, J. Catal. 227 (2004) 164.
[16] G.D. Pirngruber, J.D. Grunwald, P.K. Roy, J.A. van Bokhoven, O. Safonova, P. Glatzal, Catal. Today 126 (2007) 127.
[17] S.E. Malykhin, I.L. Zilberberg, G.M. Zhidomirov, Chem. Phys. Lett. 414 (2005) 434.
[18] V.V. Nikisha, B.V. Shelimov, V.A. Shvets, A.P. Griva, V.B. Kazansky, J. Catal. 28 (1973) 239.
[19] K. Aika, J.H. Lunsford, J. Phys. Chem. 81 (1977) 1393.
[20] M. Che, A.J. Tench, Adv. Catal. 31 (1982) 77.
[21] M. Iwamoto, I. Hirata, K. Matsukami, S. Kagawa, J. Phys. Chem. 87 (1983) 903.
[22] K.A. Dubkov, V.I. Sobolev, G.I. Panov, Kinet. Katal. 39 (1998) 79.
[23] M.A. Rodkin, V.I. Sobolev, K.A. Dubkov, N.H. Watkins, G.I. Panov, Stud. Surf. Sci. Catal. 130 (2000) 875.
[24] P.P. Knops-Gerrits, W.J. Smith, Stud. Surf. Sci. Catal. 130 (2000) 3531.
[25] P.P. Knops-Gerrits, W.A. Goddard III, J. Mol. Catal. 166 (2001) 135.
[26] G.I. Panov, A.K. Uriarte, M.A. Rodkin, V.I. Sobolev, Catal. Today 41 (1998) 365.
[27] V.S. Chernyavsky, L.V. Pirutko, A.K. Uriarte, A.S. Kharitonov, G.I. Panov, J. Catal. 245 (2007) 466.
[28] H. Launay, S. Loridant, D.L. Nguyen, A.M. Volodin, J.L. Dubois, J.M.M. Millet, Catal. Today 128 (2007) 176;
J.M.M. Millet, I.C. Marku, J.M. Herrmann, J. Mol. Catal. A 226 (2005) 111.
[29] A. Costine, T. O'Sullivan, B.K. Hodnett, Catal. Today 99 (2005) 199.
[30] A.L. Yakovlev, G.M. Zhidomirov, R.A. van Santen, J. Phys. Chem. B 105 (2001) 12297.
[31] J.A. Ryder, A.K. Chakraborty, A. Bell, J. Catal. 220 (2003) 84;
J.A. Ryder, A.K. Chakraborty, A. Bell, J. Phys. Chem. B 106 (2002) 7059.
[32] N.A. Kachurovskaya, G.M. Zhidomirov, R.A. van Santen, J. Phys. Chem. B 108 (2004) 5944.
[33] B.R. Wood, J.A. Reimer, A. Bell, M.T. Janicke, K.C. Ott, J. Catal. 224 (2004) 148;
B.R. Wood, J.A. Reimer, A. Bell, M.T. Janicke, K.C. Ott, J. Catal. 225 (2004) 302.
[34] K. Yoshizawa, Y. Shiota, T. Yumura, T. Yamabe, J. Phys. Chem. B 104 (2000) 734.
[35] M. Mauvezin, G. Delahay, B. Coq, S. Kieger, J.C. Jumas, J. Olivier-Fourcade, J. Phys. Chem. B 105 (2001) 928.
[36] T. Osch, T. Turek, Chem. Eng. Sci. 54 (1999) 4513.
[37] G. Berlier, A. Zecchina, G. Spoto, G. Ricchiardi, S. Bordiga, C. Lamberti, J. Catal. 215 (2003) 264.
[38] L. Kiwi-Minsker, D.A. Bulushev, A. Renken, J. Catal. 219 (2003) 273.
[39] I. Yuranov, D. Bulushev, A. Renken, L. Kiwi-Minsker, Appl. Catal. 319 (2006) 128.
[40] G.D. Pirngruber, J. Catal. 219 (2003) 456;
G.D. Pirngruber, M. Luechinger, P.K. Roy, A. Cecchetto, P. Smirniotis, J. Catal. 224 (2004) 429.
[41] A.M. Volodin, G.M. Zhidomirov, K.A. Dubkov, E.J.M. Hensen, R.A. van Santen, Catal. Today 110 (2005) 247.
[42] E.V. Kondratenko, J. Perez-Ramirez, Appl. Catal. B 64 (2006) 35.
[43] K. Sun, H. Zhang, H. Xia, Y. Lian, Y. Li, Z. Feng, P. Ying, C. Li, Chem. Commun. (2004) 2480.
[44] K. Sun, H. Xia, E. Hensen, R. van Santen, C. Li, J. Catal. 238 (2006) 186.
[45] G.D. Pirngruber, P.K. Roy, R. Prins, Phys. Chem. Chem. Phys. 8 (2006) 3939;
G.D. Pirngruber, P.K. Roy, R. Prins, J. Catal. 246 (2007) 147.
[46] K.S. Pillai, J. Jia, W.M.H. Sachtler, Appl. Catal. A Gen. 264 (2004) 133.
[47] J. Perez-Ramirez, F. Kapteijn, G. Mul, J.A. Moulijn, Catal. Commun. 3 (2002) 19.
[48] J. Novakova, M. Lhotka, Z. Tvaruzkova, Z. Sobalik, Catal. Lett. 83 (2002) 215;
J. Novakova, M. Lhotka, Z. Tvaruzkova, Z. Sobalik, Catal. Lett. 89 (2004) 123.
[49] J. Novakova, Z. Sobalik, Catal. Lett. 105 (2005) 169.
[50] A. Zecchina, M. Rivallan, G. Berlier, C. Lamberti, G. Ricchiardi, Phys. Chem. Chem. Phys. 9 (2007) 3483.
[51] E.M. El-Malki, R.A. van Santen, W.M.H. Sachtler, J. Catal. 196 (2000) 212.

[52] Q. Zhu, E.J.M. Hensen, B.L. Mojet, J.H.M.C. van Wolputa, R.A. van Santen, Chem. Commun. (2002) 1232.
[53] G.D. Pirngruber, P.K. Roy, Catal. Today 110 (2005) 199.
[54] A. Heyden, B. Peters, A. Bell, F.J. Keil, J. Phys. Chem. B 109 (2005) 1857.
[55] D.A. Bulushev, P.M. Prechtl, A. Renken, L. Kiwi-Minsker, Ind. Eng. Chem. Res. 46 (2007) 4178.
[56] K.A. Dubkov, E.V. Starokon, E.A. Paukshtis, A.M. Volodin, G.I. Panov, Kinet. Catal. 45 (2004) 202.
[57] G.I. Panov, K.A. Dubkov, Ye.A. Paukshtis, in: G. Centi, B. Wichterlova, A. Bell (Eds.), Catalysis by Unique Metal Ion Structures in Solid Matrices, in: NATO Science Series, Kluwer Academic, 2001, p. 149.
[58] J. Valyon, W.K. Hall, J. Phys. Chem. 97 (1993) 7054.
[59] H. Einaga, A. Ogata, S. Futamura, T. Ibusuki, Chem. Phys. Lett. 338 (2001) 303.
[60] T. Berger, M. Sterrer, O. Diwald, E. Knözinger, D. Panayotov, T.L. Thompson, J.T. Yates Jr., J. Phys. Chem. B 109 (2005) 6061.
[61] M.J. Filatov, G.L. Elizarova, O.V. Gerasimov, G.M. Zhidomirov, V.N. Parmon, J. Mol. Catal. 91 (1994) 71.
[62] G.L. Elizarova, G.M. Zhidomirov, V.N. Parmon, Catal. Today 58 (2000) 71.
[63] W. Ruttinger, G.C. Dismukes, Chem. Rev. 97 (1997) 1.
[64] T. Ohno, D. Haga, K. Fujihara, K. Kaizaki, M. Matsumura, J. Phys. Chem. B 101 (1997) 6415.
[65] G.R. Bamwendaa, T. Uesigi, Y. Abe, K. Sayama, H. Arakawa, Appl. Catal. A 205 (2001) 117.
[66] M. Ni, M.K.H. Leung, D.Y.C. Leung, K. Sumathy, Renew. Sustain. Energy Rev. 11 (2007) 401.
[67] B.T. Luke, J.R. Collins, G.H. Loew, A.D. McLean, J. Am. Chem. Soc. 112 (1990) 8686.